TU/e EINDHOVEN UNIVERSITY OF TECHNOLOGY

Very early disease manifestations of macular telangiectasia type 2

Citation for published version (APA):
Issa, P. C., Heeren, T. F. C., Kupitz, E. H., Holz, F. G., & Berendschot, T. T. J. M. (2016). Very early disease manifestations of macular telangiectasia type 2. *Retina : the Journal of Retinal and Vitreous Diseases*, *36*(3), 524-534. https://doi.org/10.1097/IAE.0000000000000863

Document license:
TAVERNE

DOI:
10.1097/IAE.0000000000000863

Document status and date:
Published: 01/03/2016

Document Version:
Publisher's PDF, also known as Version of Record (includes final page, issue and volume numbers)

Please check the document version of this publication:

• A submitted manuscript is the version of the article upon submission and before peer-review. There can be important differences between the submitted version and the official published version of record. People interested in the research are advised to contact the author for the final version of the publication, or visit the DOI to the publisher's website.
• The final author version and the galley proof are versions of the publication after peer review.
• The final published version features the final layout of the paper including the volume, issue and page numbers.

Link to publication

General rights
Copyright and moral rights for the publications made accessible in the public portal are retained by the authors and/or other copyright owners and it is a condition of accessing publications that users recognise and abide by the legal requirements associated with these rights.

• Users may download and print one copy of any publication from the public portal for the purpose of private study or research.
• You may not further distribute the material or use it for any profit-making activity or commercial gain
• You may freely distribute the URL identifying the publication in the public portal.

If the publication is distributed under the terms of Article 25fa of the Dutch Copyright Act, indicated by the "Taverne" license above, please follow below link for the End User Agreement:

www.tue.nl/taverne

Take down policy
If you believe that this document breaches copyright please contact us at:

openaccess@tue.nl

providing details and we will investigate your claim.

Download date: 16. Nov. 2023

VERY EARLY DISEASE MANIFESTATIONS OF MACULAR TELANGIECTASIA TYPE 2

PETER CHARBEL ISSA, MD, DPHIL,* TJEBO F. C. HEEREN, MD,* ELKE H. KUPITZ, MD,* FRANK G. HOLZ, MD,* TOS T. J. M. BERENDSCHOT, PHD†

Background: To report very early morphologic and functional alterations in patients with macular telangiectasia type 2.

Methods: Patients with asymmetric disease manifestations, in whom retinal alterations characteristic for macular telangiectasia type 2 were present in one but not in the apparently unaffected fellow eye, underwent multimodal imaging and functional testing (microperimetry, visual acuity, reading ability, Amsler test).

Results: Fellow eyes not allowing the diagnosis of macular telangiectasia type 2 based on hitherto diagnostic standards consistently showed a severely reduced directional cone reflectance (Stiles–Crawford effect). Optical coherence tomography revealed an asymmetric configuration of the foveal pit with focal temporal thinning most pronounced at 1° eccentricity. Topographically related, macular pigment optical density was reduced in a small wedge-shaped temporal paracentral sector, resulting in an increased signal on fundus autofluorescence and fluorescein angiography imaging. No functional deficits were detectable in fellow eyes. Haidinger brushes were perceived in the fellow eye but not in the affected index eye with pronounced loss of macular pigment.

Conclusion: Specific morphologic alterations precede vascular alterations and functional deficits in macular telangiectasia type 2. The described alterations indicate a primarily degenerative process with a secondary retinal vascular phenotype, and may be helpful for early identification of patients and affected family members.

RETINA 36:524–534, 2016

Macular telangiectasia (MacTel) type 2 is a progressive degenerative retinal disease with specific vascular alterations affecting an oval region at the posterior pole.[1] Funduscopy may reveal characteristic features such as retinal graying, blunted retinal venules, crystalline superficial retinal deposits and in later disease stages intraretinal pigment plaques and retinal atrophy.[1] However, all these alterations may either be absent or very subtle in early disease stages.

Advanced retinal imaging technology has been useful in identifying characteristic morphologic alterations in MacTel type 2 that may remain undetected by clinical examination and/or fundus photography only. Findings include leaking ectatic capillaries on fluorescein angiography (Fl-A), atrophic alterations of the retina on optical coherence tomography (OCT), and a characteristic loss of macular pigment detectable on fundus autofluorescence (AF) imaging.[1–4]

Although eponymous, it has been suggested that the vascular disease manifestations might occur secondarily to a degenerative disease process of the neurosensory retina. For instance, the areas of macular pigment loss as well as of changes visible on OCT analysis typically exceed the area affected by vascular alterations.[5,6] Such analysis has largely been performed in disease stages where Fl-A readily allowed the diagnosis of MacTel type 2. However, the morphologic changes at disease initiation have not been investigated in detail, possibly because the diagnosis is frequently delayed until well-known and characteristic retinal changes have developed, and because the disease

From the *Department of Ophthalmology, University of Bonn, Bonn, Germany; and †University Eye Clinic Maastricht, Maastricht, the Netherlands.

Supported by the ProRetina Deutschland, Aachen, Germany. The Department of Ophthalmology, University of Bonn, is a clinical center of the MacTel study funded by the Lowy Medical Research Institute, La Jolla. The Department of Ophthalmology, University of Bonn, receives imaging devices from Heidelberg Engineering.

Presented in part at the annual meeting of the Association for Research in Vision and Ophthalmology, Seattle, May 2013.

None of the authors have any financial/conflicting interests to disclose.

P. Charbel Issa and T. F. C. Heeren contributed equally to this work.

Reprint requests: Peter Charbel Issa, MD, DPhil, Department of Ophthalmology, University of Bonn, Ernst-Abbe-Str. 2, 53127 Bonn, Germany; e-mail: peter.issa@ukb.uni-bonn.de

Copyright © by Ophthalmic Communications Society, Inc. Unauthorized reproduction of this article is prohibited.

may remain asymptomatic until later disease stages have ensued.[7]

Recognition of the disease in its earliest stage is desirable to gain further insight into the disease pathophysiology and natural history, to develop future staging schemes, and to identify disease carriers with an asymptomatic or very early disease manifestation. The latter may be important for studies aiming at identifying possible genetic factors. Also, early diagnosis of the disease may become relevant to preserve vision once treatment options become available. Once vision loss has developed, it is usually progressive.[8] Thus, potential future therapies may at best modify further functional decline if initiated in later disease stages, limiting the potential benefit of therapeutic approaches such as neuroprotection.[9]

Herein, we used a multimodal imaging approach and extensive functional testing to identify the earliest morphologic and functional alterations in patients with MacTel type 2. Patient inclusion was based on an asymmetric disease manifestation where only one eye clearly allowed the diagnosis based on hitherto diagnostic criteria, whereas the other did not.

Methods

Patient Selection

Patients were selected from a single center cohort of 137 patients with MacTel type 2 at the Department of Ophthalmology, University of Bonn, Germany. Assuming a generally bilateral presentation of MacTel type 2, patients with the most asymmetric disease manifestation were selected from the database. The diagnosis was based on characteristic findings in the more severely affected eye on funduscopy, Fl-A, macular pigment mapping, and OCT scanning.[1] To be included in this study, an additional requirement was that the fellow eye should not show characteristic signs for MacTel type 2 on funduscopy and should not allow a clear diagnosis on Fl-A and OCT imaging when investigated by two retinal specialists (P.C.I. and T.F.C.H.). All included patients were examined prospectively by ophthalmoscopy, various additional retinal imaging procedures, and functional testing (overview provided in Table 1). All imaging (except reflectometry, see below) and functional assessments were performed by T.F.C.H. or P.C.I. Interobserver variability was not assessed.

The study was conducted in accordance with the Declaration of Helsinki and was approved by the local research ethics committee (University of Bonn, Germany). Informed consent was obtained from all participants.

Imaging Procedures

All retinal imaging was performed after dilating the pupil with tropicamide 0.5% and phenylephrine 2.5% eye drops. Digital color fundus images were acquired using a Visucam 500 (Carl Zeiss Meditec AG, Jena, Germany). Fluorescein angiography, fundus AF, and spectral domain OCT were recorded using an instrument combining a confocal scanning laser ophthalmoscope with an OCT device (Spectralis HRA-OCT; Heidelberg Engineering, Heidelberg, Germany).[10]

Fluorescein angiography and AF images with improved signal-to-noise ratio were recorded using the automatic real-time mode, which is able to track slight movements of the fundus based on fundus landmarks with high contrast and thus allows averaging up to 100 consecutive frames in real time. Single-averaged Fl-A and AF images were recorded centered on the anatomical fovea with an intensity resolution of 8 bits/pixel and a 1536 × 1536 pixel resolution (high-resolution mode). For quantitative analysis of AF images, nonnormalized images were recorded. Normalized AF images (i.e., automatic software enhancement of contrast by histogram stretching) were used for qualitative illustrations of disease-related alterations.

Horizontal 30° single OCT B-scans were recorded in the high-speed mode with 768 A-scans per B-scan and a lateral digital resolution of 11 μm/pixel. Macular OCT thickness maps (15 × 10°) were calculated from

Table 1. Overview on Morphologic and Functional Testing

Retinal Imaging and Reflectometry	Functional Testing
Fundus photography	Best-corrected visual acuity
Fundus autofluorescence	Reading ability
Macular pigment mapping	Perception of metamorphopsia
Fluorescein angiography	Microperimetry
Spectral domain OCT	Haidinger brushes
Reflectometry	
Stiles-Crawford effect	
MPOD	

OCT, optical coherence tomography; MPOD, macular pigment optical density.

Copyright © by Ophthalmic Communications Society, Inc. Unauthorized reproduction of this article is prohibited.

97 consecutive horizontal 15° B-scans (~30 μm distance between individual B-scans) recorded in the high-resolution mode with 768 A-scans per B-scan and a lateral digital resolution of 5 μm/pixel. The automatic real-time mode was used to improve the signal-to-noise ratio, averaging up to 100 consecutive frames for single-scan recordings and 9 frames to record data sets for calculating thickness maps.

Distribution of macular pigment optical density (MPOD) was assessed as described previously using a modified 2-wavelenghts HRA classic (Heidelberg Engineering).[3,11] In brief, MPOD was calculated from two averaged fundus AF images (each consisting of up to 16 single images) derived from excitation using 488 nm and 514 nm light, respectively, in conjunction with a barrier filter that blocks wavelengths shorter than 560 nm. Because of the maximum absorbance of macular pigment at 460 nm, the AF signal recorded using 488 nm excitation light is strongly dependent on macular pigment density, whereas the AF signal of the 514 nm AF image is not. Subtraction of the two averaged images results in an image representing MPOD distribution, which was saved with an intensity resolution of 8 bits/pixel, and a 512 × 512 pixel resolution.

For comparison with normative data, 10 control subjects of similar age (mean ± SD, 65 ± 5.9 years; range, 53–74 years) without any history of or evidence for retinal disease on funduscopy, fundus AF, MPOD mapping, and OCT scanning underwent the same noninvasive imaging protocol.

Image Analysis

The high variability of the normal foveal configuration, MPOD, and the resulting appearance on AF images would not allow detecting differences of absolute values compared with controls when investigating low case numbers. Based on the assumption of a low interindividual variability of the symmetry between the corresponding temporal and nasal eccentricities, symmetry of retinal thickness profiles, macular pigment distribution, and signal intensity on AF images was analyzed by one of the authors (T.F.C.H.; Figure 1).

Thickness maps were centered on the anatomical foveal center, which was defined by the largest distance between the two outer highly reflective layers on single OCT scans.[7] The same landmark was used to identify the foveal center on single horizontal OCT scans. Retinal thickness was measured between the outer border of the highly reflective retinal pigment epithelial band and the inner limiting membrane using the HEYEX software, version 5.7a (Heidelberg Engineering). Derived measurements for each A-scan were extracted and plotted up to an eccentricity of 5° nasally and temporally. Nasal measurements were subtracted from temporal values at corresponding eccentricity (Figure 1A). This resulted in a thickness difference curve (temporal–nasal) plotted against eccentricity.

A similar approach was applied for the analysis of the MPOD and AF symmetry. Images were analyzed using ImageJ software (version 1.47; National Institutes of Health, Bethesda, MD; http://rsb.info.nih.gov/ij). After applying a standard Gaussian blur with a 3.5-pixel radius (σ) to reduce image noise, the mean gray level profile within a 1° broad horizontal band (equivalent to 51 pixels on fundus AF images and 17 pixels on MPOD images) was plotted through the foveal center extending 5° both temporally and nasally (equivalent to 512 and 170 pixels on fundus AF and MPOD images, respectively). Again, nasal values were subtracted from

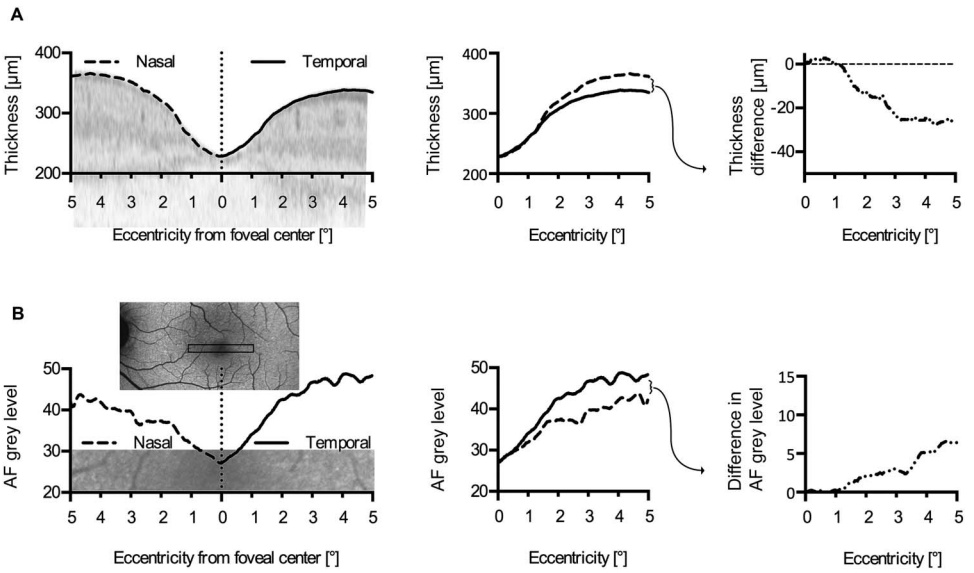

Fig. 1. Strategy for analyzing foveal symmetry on OCT (**A**) and scanning laser ophthalmoscope images (**B**). **A.** Left: horizontal thickness profile of the central 10°. **A.** Middle: thickness measurements at equivalent eccentricities were subtracted (temporal-nasal). **A.** Right: resulting thickness difference curve used for analysis. **B.** A similar approach was used for analysis of symmetry on fundus AF and macular pigment images. **B.** Left and middle: Instead of a thickness profile, a gray level plot profile (middle) along a central 1 × 10° bar (left) was plotted. Grey level measurements at equivalent eccentricities were subtracted (temporal-nasal). **B.** Right: resulting gray level difference curve used for analysis.

Copyright © by Ophthalmic Communications Society, Inc. Unauthorized reproduction of this article is prohibited.

temporal values at corresponding eccentricity, resulting in a gray level difference profile (temporal–nasal) plotted against eccentricity (Figure 1B).

Reflectometry

Reflectometry recordings and data analysis were all performed by T.T.J.M.B. The foveal reflection analyzer was used to measure the cone-specific directional reflectance. A prototype foveal reflection analyzer was detailed by Zagers et al[12]; the present version was described by van de Kraats and van Norren[13]. Reflection was measured at the fovea and at eccentricities of 1, 2, 3, and 4° along a horizontal line through the foveal center. In every included eye, at least three measurements were performed for each eccentricity at the optimal pupil position, that is, the optical Stiles–Crawford peak (for an extensive description of the measurement routine, see van de Kraats and van Norren[13]).

The spectra were analyzed with an updated version[13,14] of the original[15] van de Kraats fundus reflectance model. The model describes the spectral aspects of light reflected from the fundus for all positions in the pupil (corresponding to various incident angles at the retina) using a limited number of absorbing and reflecting layers. In short, the incoming light is thought to be reflected from four layers: the inner limiting membrane (R_{ILM}), the discs in the outer segments of the cone photoreceptors (R_d), the pigment epithelium, and the choroid. In the model, the light traveling through the eye is absorbed by four layers in the eye with known spectral characteristics: media, macular pigment (D_{MP}), melanin (D_{MEL}), and a blood layer. The lutein and zeaxanthin optical densities that make up the macular pigment were both fitted separately.[16] The light conditions were such that all photopigments were bleached. In the optical model, the densities of these absorbers and the reflectances at the interfaces are optimized to fit the measured spectral reflectance. The recent version of the model simultaneously fits the directional reflection from the cone receptors (optical Stiles–Crawford effect, SCE) and the nondirectional reflection from more anterior and posterior layers in a wavelength range of 400 nm to 950 nm.

To make the model more robust, we fixed a number of minimally age-dependent parameters[13] as described in other studies using this technique.[17,18] This applied to ρ, a measure for the steepness of the optical SCE in the pupil plane, that was fixed at 0.149[13] and D_{RL}, a measure for the amount of Rayleigh scatter losses, that was fixed at 0.77.[14] In addition, the optical densities of the lens were given age estimates from literature.[19] The peak position of the SCE was assumed to be the same for all measurements in a particular subject, that is, for all retinal eccentricities in both eyes. It did, however, differ between different subjects. Finally, at each retinal eccentricity, eye-specific parameters were obtained by averaging the model outcomes at that position.

The main parameter in this analysis was the reflection at the cone photoreceptor layer.[13] This parameter can be used to quantify the SCE[20–24] and is a sensitive measure for detecting cone photoreceptor disturbances.[25] Normal values for this reflection as a function of retinal eccentricity were obtained from Berendschot et al[14] as well as the spatial distribution of the MPOD. The age dependency of the reflection at the cone photoreceptor layer was obtained from 53 healthy subjects ranging from 19 years to 76 years.[13] The MPOD is assumed to be age independent.[26]

Functional Testing

Best-corrected distance visual acuity was measured by standard Early Treatment Diabetic Retinopathy Study protocols with a distance chart transilluminated with a chart illuminator.

Fundus-controlled microperimetry (MP1; Nidek Technologies, Padova, Italy) was performed as described previously.[8,27,28] Test stimuli (Goldman III size, 100 milliseconds projection time, 4–2 staircase test strategy) were projected in a 16° macula test pattern with a red cross (2° in diameter) as fixation target. A high-density test grid with testing points equally spaced 1° apart covered an area of 8° horizontally and 4° vertically centered on the foveal center.

Reading performance was tested using standardized Radner reading charts as described previously.[29,30] The critical print size was set at the smallest print size that could be read with maximum reading speed. The maximum reading speed was the best reading speed in words per minute (wpm) achieved in the test. Reading acuity was determined as the smallest print size in which the patient was able to read a sentence completely in less than 20 seconds and was expressed in terms of logRAD (logarithm of Reading Acuity Determination, which is the reading equivalent of logMAR). Eyes were tested individually with the fellow eye occluded.

Metamorphopsia were assessed using Amsler grids according to a standardized protocol at reading distance.[31] Plates number 1,2 (1° grid) and 7 (more sensitive central 0.5° grid) as originally described by Amsler were used.[32,33]

Perception of Haidinger brushes was tested using the Macular Integrity Tester 2 (MIT-2; Bernell, Mishawaka, IN). This handheld device is equipped with a rotating polarization filter. Patients were asked to look into the sky through the rotating filter with each eye individually and to report if they perceived

Copyright © by Ophthalmic Communications Society, Inc. Unauthorized reproduction of this article is prohibited.

a beforehand described propeller-like figure that moves with their viewing direction.

Results

Five patients with a mean age of 69 years (SD: ±3.2) were identified in whom only one eye showed the characteristic features of MacTel type 2 (Figure 2A), whereas the fellow eye on its own would not allow the diagnosis following hitherto diagnostic standards (Figure 2B). Descriptive data of the patients included in this study are shown in Table 2. The more affected (diagnostic) eyes showed alterations compatible with disease Stages 1 to 5. Functional impairment in these

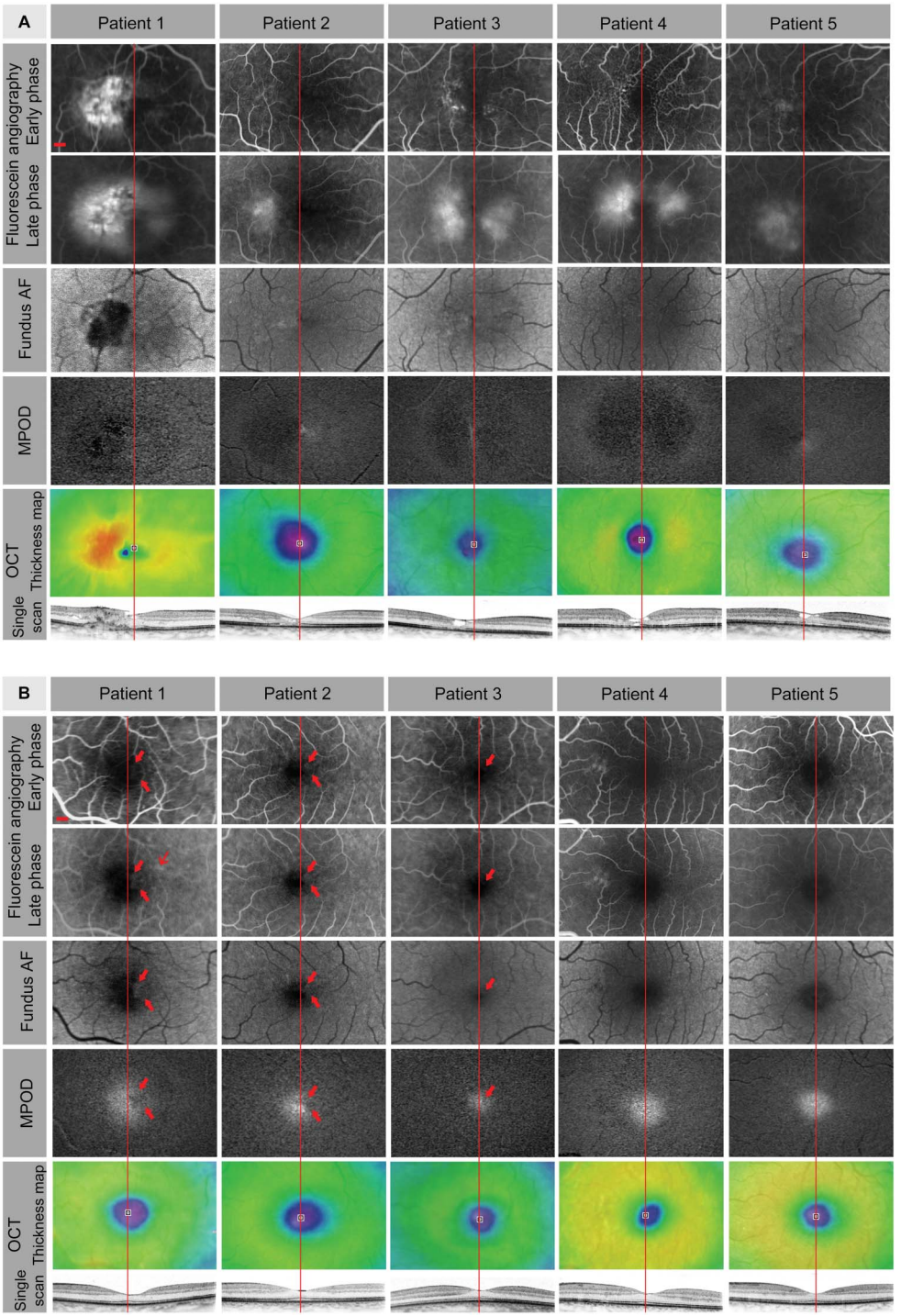

Fig. 2. Retinal images of clearly affected (**A**) and their fellow (**B**) eyes in five patients with very asymmetric MacTel type 2. **A.** One eye allowed the diagnosis based on characteristic findings on retinal imaging, including leaking macular capillaries, foveal atrophic changes on OCT scans and central depletion of macular pigment. **B.** Morphologic findings in fellow eyes with very early disease manifestation. Thick arrows (Patients 1–3) mark a sector with focally reduced macular pigment (fourth row), resulting in increased signal detection on fluorescein angiography and fundus AF images. The thin arrow (Patient 1) points out an area of minor retinal capillary leakage at approximately 2 to 3° eccentricity temporal to the foveal center. All five eyes with a very early disease stages showed temporal enlargement, thinning, and asymmetry of the foveal depression detected by spectral domain OCT macular thickness mapping. The red line represents the foveal center. AF, autofluorescence; MPOD, macular pigment optical density.

Copyright © by Ophthalmic Communications Society, Inc. Unauthorized reproduction of this article is prohibited.

Table 2. Descriptive Summary of Patients With Very Asymmetric Macular Telangiectasia type 2

Patient			Diagnostic Eye				Fellow Eye			
No.	Sex	Age (years)	BCVA	Stage*	Side	CPS	BCVA	Stage*	Side	CPS
1	M	73	20/200	5	OD	1.4	20/20	0	OS	0.5
2	F	64	20/50	2	OD	0.7	20/16	0	OS	0.3
3	M	70	20/25	2	OD	0.8	20/20	0	OS	0.2
4	M	69	20/50	3	OD	0.7	20/16	0	OS	0.1
5	M	69	20/32	1	OD	0.6	20/13	0	OS	0.3

Only one eye showed characteristic diagnostic signs, whereas the fellow eye was seemingly normal.
*Disease Stages 1 to 5 according to Gass and Blodi. Stage 0 reflects absence of typical disease signs.
CPS, critical print size (logRAD, minimum print size with the average reading speed).
BCVA, best-corrected distance visual acuity; F, female; M, male; OD, right eye; OS, left eye.

eyes included reduced best-corrected visual acuity, paracentral scotomata, a disproportionate reduced reading ability (e.g., in Patient 3; Table 2), metamorphopsia, and nonperception of Haidinger brushes.

The following analysis of functional and morphologic alterations focuses on findings in the seemingly unaffected fellow eyes, except where explicitly stated.

Functional Alterations

No patient reported visual symptoms in the fellow eye. All seemingly unaffected fellow eyes had a best-corrected visual acuity of 20/20 or better, a normal retinal sensitivity assessed by microperimetry, and a reading ability comparable with normal (Table 2).[30] Only Patient 1 revealed a moderately reduced reading performance, which may be because of the slightly more pronounced retinal alterations compared with the other patients or to an overall lower reading competence. Each patient perceived Haidinger brushes with the fellow eye, and there was no perception of metamorphopsia. Thus, overall functional performance in fellow eyes was not different from normal.

Morphologic Alterations

Based on hitherto diagnostic standards, no abnormalities suggestive for the presence of MacTel type 2 were detected either funduscopically or on fundus photographs. Qualitative assessment of Fl-A and fundus AF revealed a faintly increased signal within a paracentral temporal wedge-shaped sector in 3 of the 5 fellow eyes (Figure 2B, rows 1–3, Patients 1–3, thick arrows). This hyperfluorescence on Fl-A did not increase in size or fluorescence intensity in the late angiographic phase, thus largely excluding a leakage or staining phenomenon. In addition, one eye showed some mild leakage at approximately 2 to 3° eccentricity temporal to the foveal center (Figure 2B, Patient 1, thin arrow) and, thus, could be classified as Stage 1 disease, at least in the context with the other clearly affected eye.

Macular pigment distribution maps revealed a small paracentral area with loss of macular pigment in 3 of the 5 eyes (Figure 2B, row 4, Patients 1–3, thick arrows). The wedge-shaped area was topographically related to the faint increased signal on Fl-A and AF imaging. This suggests a window defect within the normally round and symmetric masking of the foveal fundus AF and Fl-A signal due to focal loss of macular pigment (which absorbs the blue excitation light used for fundus AF and Fl-A imaging).

The OCT recordings revealed an asymmetric foveal dip in all fellow eyes, with the thinnest area slightly displaced temporally from the foveal center (Figure 2B, rows 5–6). There were otherwise none of the characteristic features observed in later disease stages, such as hyporeflective cavities, an obvious loss of the inner segment/outer segment band (ellipsoid zone) integrity, or marked thinning of the photoreceptor layer.

Quantitative analysis of symmetry about the foveal center confirmed differences between the seemingly unaffected fellow eyes and controls. This difference was largest at 1° eccentricity (Figure 3). In line with the qualitative findings, fellow eyes revealed a lower thickness, reduced macular pigment, and an increased AF signal temporally to the foveal center. The effect was most consistent on OCT analysis, where all fellow eyes were outside the 95% confidence interval of controls. More peripherally at 4 and 5° eccentricity, MPOD appeared to be slightly higher temporally, whereas OCT and AF measurements approximated control levels.

Reflectometry revealed severely reduced directional cone reflectance (SCE) in all fellow eyes (Figure 4, upper graphs). Although the difference from controls on the other imaging modalities appeared most pronounced temporal to the foveal center at 1° eccentricity, reduced reflectance was also observed in the central and nasal measurements. At the same time, MPOD measurements derived from the same reflectometry data revealed MPOD levels within the normal range (Figure 4, lower graphs), confirming the reliability of the reflectometry recordings. The more affected (diagnostic) eyes all

Copyright © by Ophthalmic Communications Society, Inc. Unauthorized reproduction of this article is prohibited.

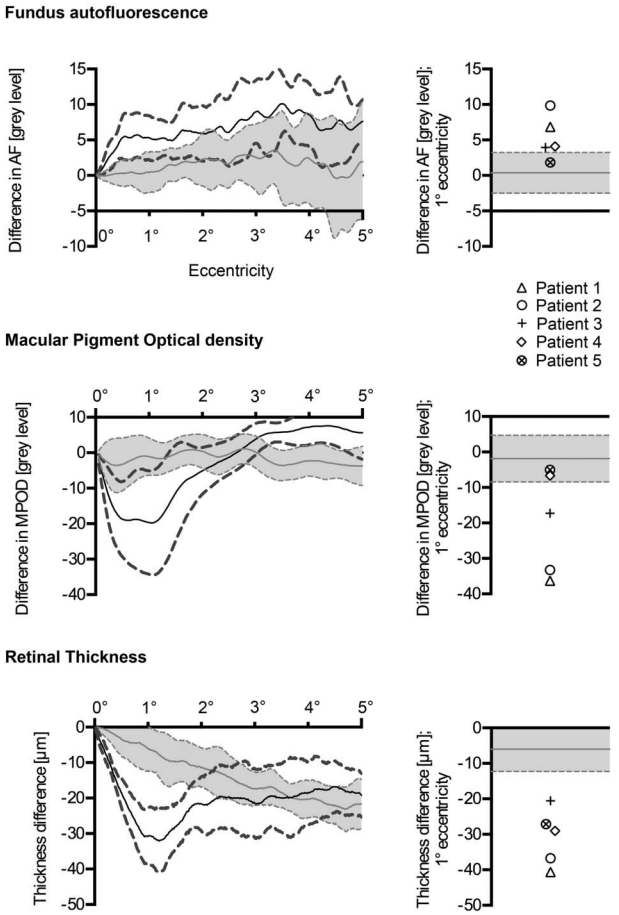

Fig. 3. Quantitative analysis of foveal asymmetry in very early disease manifestation of MacTel type 2. Left graphs show the mean difference (black continuous line) ± SD (black dashed lines) between nasal and temporal measurements of fundus autofluorescence (AF; upper), macular pigment optical density (MPOD; middle), and retinal thickness (bottom) as described in Figure 1. The gray area represents the mean ± SD measurements in normal controls. The right graphs show individual asymmetry measurements at an eccentricity of 1°, where difference profiles revealed the most pronounced asymmetry in eyes with early MacTel type 2. Asymmetry at this eccentricity was most consistent on OCT analysis.

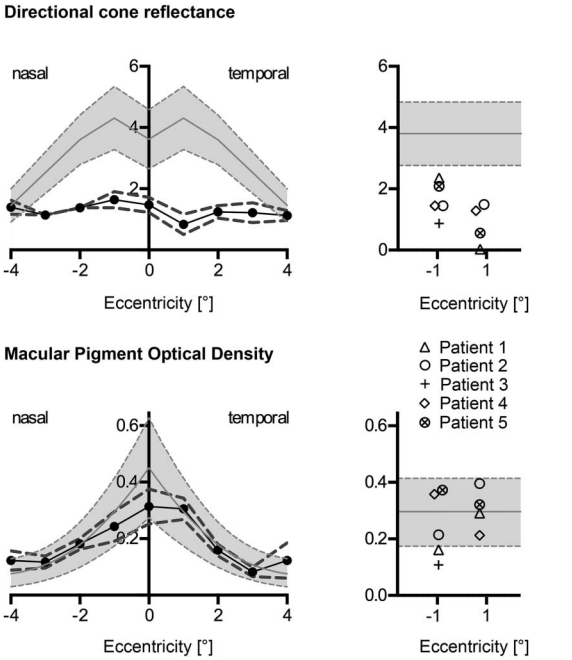

Fig. 4. Directional cone reflectance (%; Stiles-Crawford effect) and macular pigment optical density (MPOD) assessed using reflectometry in very early manifestation of MacTel type 2. Measurements were performed along a horizontal line through the fovea at 1° intervals up to an eccentricity of 4° (left graphs; mean ± SD; all lines between data points drawn as a guide to the eye). Right graphs illustrate measurements for each fellow eye at 1° nasally and temporally. Measurements for Patient 3 at 1° temporally were not reliable and are therefore not reported. Grey areas represent mean ± SD measurements in controls, accounting for the age dependency (see Methods section).

showed almost absent directional cone reflectance and subnormal MPOD (not shown).

Very Early Disease Manifestations in Family Members

Thirty-one first-degree family members of patients with MacTel type 2 were investigated, including 16 children (age, mean ± SD, 42.6 ± 11.7 years; range, 20–56 years) and 15 siblings (age, mean ± SD, 60.1 ± 14.0 years; range, 34–76 years). No family member showed signs that have as yet been diagnostic for MacTel type 2. However, one 46-year-old son (Figure 5; family member 1) and one 66-year-old monozygotic twin (Figure 5; family member 2) of two index patients revealed an asymmetric foveal pit in both eyes as described above. There was also a small wedge-shaped loss of macular pigment along with a topographically related slightly increased signal on AF imaging in the right eye of family member 1 and both eyes of family member 2 (Figure 5; thick arrows). A minor leakage was detectable on Fl-A temporal to the fovea in one eye of each family member (Figure 5, thin arrows). Reflectometry in the two family members revealed borderline low MPOD levels and a directional cone reflectance below normal in both eyes (Figure 6).

Discussion

In this study, patients with a markedly asymmetric disease manifestation of MacTel type 2 were investigated to identify the earliest or minimal disease-related morphologic and functional alterations in the seemingly unaffected eye. This approach assumes a generally bilateral occurrence of a disease typically characterized by rather symmetric manifestation. In case purely unilateral MacTel type 2 would exist, our findings could be explained by chance alone. However, apparently unaffected fellow eyes revealed a consistent pattern of morphologic abnormalities that are unlikely to be explained by coincidence.

Copyright © by Ophthalmic Communications Society, Inc. Unauthorized reproduction of this article is prohibited.

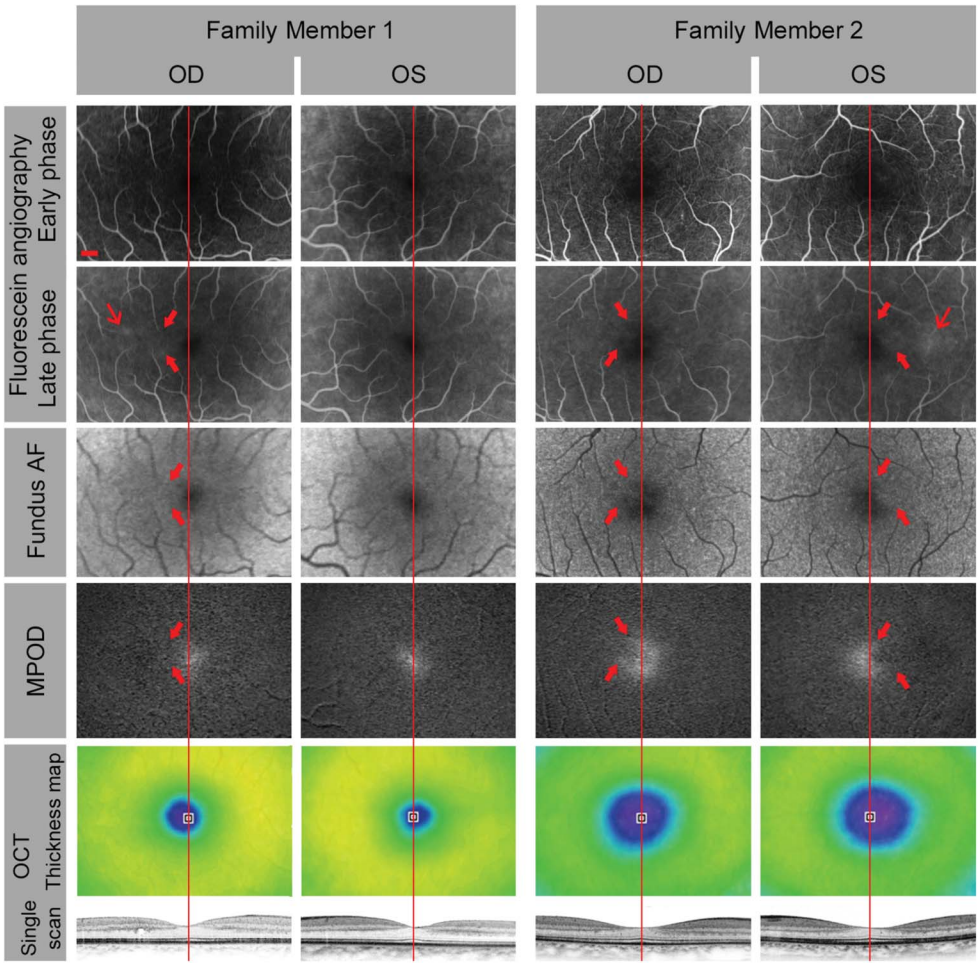

Fig. 5. Retinal images in two family members with very early signs for MacTel type 2. Thick arrows mark a sector with focally reduced macular pigment optical density (MPOD), which was most pronounced in the left eye of family member 2. This results in focally increased signal detection on fluorescein angiography and fundus autofluorescence (AF) images. The thin arrows (right eye of family member 1 and left eye of family member 2) point out an area of minor retinal capillary leakage at approximately 2 to 3° eccentricity temporal to the foveal center. Foveal asymmetry with temporal enlargement of the foveal depression on optical coherence tomography (OCT) analysis was present in all eyes. OD, right eye; OS, left eye. The red line represents the foveal center.

Reduced directional cone reflectance, asymmetry of the foveal pit, and focal loss of macular pigment were identified as minimal morphologic alterations, suggesting a primary degenerative disease process in MacTel type 2. Vascular alterations apparently develop later in the course of the disease and, thus, would represent a secondary phenomenon, as suggested in previous studies that mainly investigated patients with later disease stages.[1,5] The finding that vascular changes associated with MacTel type 2 occur secondarily may be important for understanding the mechanism of disease and may help direct future investigations toward this disease. However, the possibility remains that vascular alterations undetectable by Fl-A may cause the observed minor morphologic alterations.

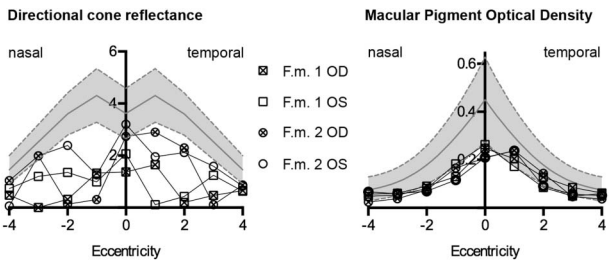

Fig. 6. Directional cone reflectance (%; Stiles-Crawford effect) and macular pigment optical density (MPOD) assessed using reflectometry in the two family members (F.m.). Measurements were performed along a horizontal line through the fovea at 1° intervals up to an eccentricity of 4° (all lines between data points drawn as a guide to the eye). The directional cone reflectance is generally reduced in both eyes of both individuals, whereas the MPOD is within the lower SD limits of healthy controls. Gray areas represent mean ± SD measurements in controls, taking into account the age dependence (see Method section). OD, right eye; OS, left eye.

Reduced directional cone reflectance may be explained by a decrease in cone density. However, such reason is unlikely as a recent study in patients with MacTel type 2 revealed a normal cone density in areas with an inconspicuous inner segment/outer segment band (ellipsoid zone) on spectral domain OCT imaging,[34] which was the case in all eyes with very early alterations. Further, an absent inner segment/outer segment may completely recover including a full recovery of the directional reflectance.[35,36] The reduced cone reflectance may otherwise be explained by a disturbed cone outer segment alignment or shape, or a decreased number of cone outer segment discs. Independent from

Copyright © by Ophthalmic Communications Society, Inc. Unauthorized reproduction of this article is prohibited.

the exact cause, the disturbed reflectance was present in all fellow eyes of patients with manifest MacTel type 2 in the other eye. Reduced directional cone reflectance most likely precedes other visible morphologic changes and functional decline since it was even altered nasal to the foveal center where all other imaging modalities showed findings within normal limits.

Other retinal structures also exhibit directional properties. The nerve fiber layer is highly directional,[37] which can be visualized by changing the angle of incidence[38] and can be used to discriminate the outer nuclear layer and Henle's fiber layer in OCT images.[39] Furthermore, the vitreous–inner limiting membrane interface shows a specular reflection that also shows up in changing the angle of incidence. However, in the foveal reflection analyzer, the entrance pupil is fixed at the optimum of the SCE. Therefore, both structures will not interfere in determining the strength of the directional reflectance of the photoreceptors.

A slightly abnormal configuration of the foveal pit was present in all eyes with early changes. The thinning of the temporal slope may cause blunting or absence of the foveolar reflex on funduscopy. Since cones and Müller cells are the only cellular elements in this retinal area, loss in number (as shown in a postmortem analysis for a later disease stage[40,41]) or volume of one of these cell types may explain temporal foveal thinning. Hyporeflective spaces characteristic for MacTel type 2 were not detected and thus seem to occur later in the disease course. The asymmetric foveal thinning may later be masked by the presence of a low-grade intraretinal edema and it may become increasingly difficult to define the foveal center (and thus assess asymmetry) in later disease stages because of progressive disorganization of the foveal anatomy.

Focal loss of macular pigment in the temporal proximity of the foveal center was topographically related to the asymmetric foveal thinning. This morphologic change was visible in 3 of 5 fellow eyes. Moreover, a mild focally increased fluorescence signal on early and late-phase angiography as well as on fundus AF imaging in the area of abnormal MPOD was detected, suggesting that its origin is not an additional fluorescent substance (such as leaking dye on Fl-A or accumulation of fluorophores on fundus AF) but rather focally reduced absorption of the excitation light by a decreased density of macular pigment. Gass and Blodi proposed a "mild staining at the level of the outer parafoveolar retina temporally" in late-phase Fl-A to be characteristic in the earliest disease stage.[42] At least in very early disease stages, this observation may rather be due to a focal "window defect" in macular pigment with increased choroidal fluorescence being detected at the level of the outer retina.[1] This should be differentiated from the characteristic fluorescein leakage in subsequent disease stages.

No functional deficit could be detected in any fellow eye with very early manifestation of MacTel type 2, indicating that anatomical alterations precede early functional alterations and symptoms as described recently.[43] We have not performed fine matrix mapping as a means to detect alterations of scotopic vision, which were previously suggested to precede declining retinal sensitivity on microperimetry testing.[44] Such testing is currently only available in few centers and might be investigated in future studies. Perception of Haidinger brushes with the fellow eyes, but not with the diagnostic eyes that revealed depletion of macular pigment characteristic for MacTel type 2, supports an important role of macular pigment for perception of this entoptic phenomenon. Of note, we can be certain about the ability of each patient to see Haidinger brushes due to the internal control with the other eye.

Very asymmetric disease manifestation is very infrequent in MacTel type 2 and was identified in less than 5% of our entire single-center patient cohort. It is possible that some patients with asymmetric presentation of MacTel type 2 remain unidentified because of dominance of the apparently unaffected eye and thus lack of visual difficulties. Occurrence of MacTel type 2 in monozygotic twins as well as in families has demonstrated a genetic component of the disease,[1,45] which would be suggestive for a rather symmetric disease manifestation. Currently, the reason for the observed asymmetry and possibly delayed disease progression in the less affected eye remains obscure as it is the case in unilateral or very asymmetric retinitis pigmentosa, macular dystrophies, and related inherited retinal diseases. The possibility remains that patients with very asymmetric disease manifestation might have a subform of MacTel type 2 that may or may not reflect the more standard disease. Thus, early changes described herein may or may not fully reflect early changes in the MacTel type 2 population as a whole.

In conclusion, reduced directional cone reflectance was the earliest and most consistent retinal alteration related to MacTel type 2 in this study. Thinning of the temporal foveal pit and a topographically related focal loss of macular pigment may subsequently be detected very early in the disease course. These findings may be useful for determining if a subject is affected or not, and show the large variability of disease manifestation even within families. Apparent unilaterality of MacTel type 2 likely represents a very asymmetric disease expression. The anatomical alterations appear to precede functional deterioration and the eponymous vascular alterations that rather represent a secondary phenomenon.

Copyright © by Ophthalmic Communications Society, Inc. Unauthorized reproduction of this article is prohibited.

Key words: asymmetry, disease staging, early changes, fundus autofluorescence, juxtafoveolar telangiectasis, macular pigment, macular telangiectasia type 2, optical coherence tomography, reflectometry.

References

1. Charbel Issa P, Gillies MC, Chew EY, et al. Macular telangiectasia type 2. Prog Retin Eye Res 2013;34:49–77.
2. Gaudric A, Ducos de LG, Cohen SY, et al. Optical coherence tomography in group 2A idiopathic juxtafoveolar retinal telangiectasis. Arch Ophthalmol 2006;124:1410–1419.
3. Charbel Issa P, van der Veen RLP, Stifjs A, et al. Quantification of reduced macular pigment optical density in the central retina in macular telangiectasia type 2. Exp Eye Res 2009;89: 25–31.
4. Helb HM, Charbel Issa P, van der Veen RLP, et al. Macular pigment density and distribution in patients with type II macular telangiectasia. Retina 2008;28:808–816.
5. Charbel Issa P, Berendschot TT, Staurenghi G, et al. Confocal blue reflectance imaging in type 2 idiopathic macular telangiectasia. Invest Ophthalmol Vis Sci 2008;49:1172–1177.
6. Barthelmes D, Gillies MC, Sutter FK. Quantitative OCT analysis of idiopathic perifoveal telangiectasia. Invest Ophthalmol Vis Sci 2008;49:2156–2162.
7. Gillies MC, Zhu M, Chew EY, et al. Familial asymptomatic macular telangiectasia type 2. Ophthalmology 2009;116: 2422–2429.
8. Heeren TF, Clemons T, Scholl HP, et al. Progression of vision loss in macular telangiectasia type 2. Invest Ophthalmol Vis Sci 2015;56:3905–3912.
9. Chew EY, Clemons TE, Peto T, et al. Ciliary neurotrophic factor for macular telangiectasia type 2: results from a phase 1 safety trial. Am J Ophthalmol 2015;159:659–666.e651.
10. Helb HM, Charbel Issa P, Fleckenstein M, et al. Clinical evaluation of simultaneous confocal scanning laser ophthalmoscopy imaging combined with high-resolution spectral-domain optical coherence tomoggraphy. Acta Ophthalmol 2010;88:842–849.
11. Trieschmann M, Heimes B, Hense HW, Pauleikhoff D. Macular pigment optical density measurement in autofluorescence imaging: comparison of one- and two-wavelength methods. Graefes Arch Clin Exp Ophthalmol 2006;244: 1565–1574.
12. Zagers NP, van de KJ, Berendschot TT, van ND. Simultaneous measurement of foveal spectral reflectance and cone-photoreceptor directionality. Appl Opt 2002;41:4686–4696.
13. van de Kraats J, van Norren D. Directional and nondirectional spectral reflection from the human fovea. J Biomed Opt 2008; 13:024010.
14. Berendschot TT, van de Kraats J, Kanis MJ, van Norren D. Directional model analysis of the spectral reflection from the fovea and para-fovea. J Biomed Opt 2010;15:065005.
15. van de Kraats J, Berendschot TTJM, van Norren D. The pathways of light measured in fundus reflectometry. Vis Res 1996; 36:2229–2247.
16. van de Kraats J, Kanis MJ, Genders SW, van Norren D. Lutein and Zeaxanthin measured separately in the living human retina by reflectometry. Invest Ophthalmol Vis Sci 2008;49:5568.
17. Kanis MJ, Wisse RP, Berendschot TT, et al. Foveal cone-photoreceptor integrity in aging macula disorder. Invest Ophthalmol Vis Sci 2008;49:2077–2081.
18. Kanis MJ, Lemij HG, Berendschot TT, et al. Foveal cone photoreceptor involvement in primary open-angle glaucoma. Graefes Arch Clin Exp Ophthalmol 2010;248:999–1006.
19. van de Kraats J, van Norren D. Optical density of the aging human ocular media in the visible and the UV. J Opt Soc Am A Opt Image Sci Vis 2007;24:1842–1857.
20. Zagers NP, Berendschot TT, van ND. Wavelength dependence of reflectometric cone photoreceptor directionality. J Opt Soc Am A Opt Image Sci Vis 2003;20:18–23.
21. Burns SA, Wu S, Delori F, Elsner AE. Direct measurement of human-cone-photoreceptor alignment. J Opt Soc Am A Opt Image Sci Vis 1995;12:2329–2338.
22. Vohnsen B, Iglesias I, Artal P. Guided light and diffraction model of human-eye photoreceptors. J Opt Soc Am A Opt Image Sci Vis 2005;22:2318–2328.
23. Westheimer G. Directional sensitivity of the retina: 75 years of Stiles-Crawford effect. Proc Biol Sci 2008;275: 2777–2786.
24. Gao W, Cense B, Zhang Y, et al. Measuring retinal contributions to the optical Stiles-Crawford effect with optical coherence tomography. Opt Express 2008;16:6486–6501.
25. DeLint PJ, Berendschot TT, van Norren D. A comparison of the optical Stiles-Crawford effect and retinal densitometry in a clinical setting. Invest Ophthalmol Vis Sci 1998;39:1519–1523.
26. Berendschot TT, van Norren D. On the age dependency of the macular pigment optical density. Exp Eye Res 2005;81:602–609.
27. Charbel Issa P, Tröger E, Finger R, et al. Structur-function correlation of the human central retina. PLoS One 2010;5:e12864.
28. Charbel Issa P, Helb HM, Rohrschneider K, et al. Microperimetric assessment of patients with type II macular telangiectasia. Invest Ophthalmol Vis Sci 2007;48:3788–3795.
29. Radner W, Obermayer W, Richter-Mueksch S, et al. The validity and reliability of short German sentences for measuring reading speed. Graefes Arch Clin Exp Ophthalmol 2002;240:461–467.
30. Finger RP, Charbel Issa P, Fimmers R, et al. Reading performance is reduced due to parafoveal scotomas in patients with macular telangiectasia type 2. Invest Ophthalmol Vis Sci 2009; 50:1366–1370.
31. Charbel Issa P, Holz FG, Scholl HPN. Metamorphopsia in patients with macular telangiectasia type 2. Doc Ophthalmol 2009;119:133–140.
32. Amsler M. L'examen qualitatif de la fonction maculaire. Ophthalmologica 1947;114:248–261.
33. Amsler M. Earliest symptoms of diseases of the macula. Br J Ophthalmol 1953;37:521–537.
34. Wang Q, Tuten WS, Lujan B, et al. Adaptive optics microperimetry and OCT images in macular telangiectasia type 2 retinal lesions show preserved function and recovery of cone visibility. Invest Ophthalmol Vis Sci 2015;56:778–786.
35. Kanis MJ, van Norren D. Delayed recovery of the optical Stiles-Crawford effect in a case of central serous chorioretinopathy. Br J Ophthalmol 2008;92:292–294.
36. Jacob J, Paques M, Krivosic V, et al. Meaning of visualizing retinal cone mosaic on adaptive optics images. Am J Ophthalmol 2015;159:118–123.e111.
37. Knighton RW, Qian C. An optical model of the human retinal nerve fiber layer: implications of directional reflectance for variability of clinical measurements. J Glaucoma 2000;9:56–62.
38. Lujan BJ, Roorda A, Knighton RW, Carroll J. Revealing Henle's fiber layer using spectral domain optical coherence tomography. Invest Ophthalmol Vis Sci 2011;52:1486–1492.
39. Lujan BJ, Roorda A, Croskrey JA, et al. Directional optical coherence tomography provides accurate outer nuclear layer and henle fiber layer measurements. Retina 2015;35:1511-1520.

Copyright © by Ophthalmic Communications Society, Inc. Unauthorized reproduction of this article is prohibited.

40. Powner MB, Gillies MC, Zhu M, et al. Loss of Müller's cells and photoreceptors in macular telangiectasia type 2. Ophthalmology 2013;120:2344–2352.
41. Powner MB, Gillies MC, Tretiach M, et al. Perifoveal Müller cell depletion in a case of macular telangiectasia type 2. Ophthalmology 2010;117:2407–2416.
42. Gass JD, Blodi BA. Idiopathic juxtafoveolar retinal telangiectasis. Update of classification and follow-up study. Ophthalmology 1993;100:1536–1546.
43. Heeren TF, Holz FG, Charbel Issa P. First symptoms and their age of onset in macular telangiectasia type 2. Retina 2014;34:916–919.
44. Schmitz-Valckenberg S, Fan K, Nugent A, et al. Correlation of functional impairment and morphological alterations in patients with group 2A idiopathic juxtafoveal retinal telangiectasia. Arch Ophthalmol 2008;126:330–335.
45. Parmalee NL, Schubert C, Figueroa M, et al. Identification of a potential susceptibility locus for macular telangiectasia type 2. PLoS One 2012;7:e24268.

Copyright © by Ophthalmic Communications Society, Inc. Unauthorized reproduction of this article is prohibited.